

# Influence of CNT-based Nanocomposites in Dynamic Performance of Redundant Articulated Robot

M. Saravana Mohan<sup>†\*</sup>  and P. S. Samuel Ratna Kumar<sup>‡</sup>

<sup>†</sup>*Dept. of Mechatronics Engineering, Kumaraguru College of Technology, Coimbatore, 641035, Tamil Nadu, India*

<sup>‡</sup>*Dept. of Mechanical Engineering, Kumaraguru College of Technology, Coimbatore, 641035, Tamil Nadu, India*

(Accepted March 26, 2020. First published online: April 30, 2020)

## SUMMARY

In this study, AA5083-reinforced multiwalled carbon nanotubes (MWCNT) nanocomposites were selected as the alternate material for a redundant articulated robot (RAR) design by varying the composition of MWCNT wt%. By assigning AA5083-reinforced MWCNT as a custom material to the parts of RAR developed by Solid Works and exported to MATLAB/SimMechanics platform to convert the model into multi-body system blocks. The dynamic parameter torque was observed utilising simulation capability in a SimMechanics second-generation environment. The simulation results inferred that AA5083 reinforced with increased wt% of MWCNT has better properties suitable for RAR design.

**KEYWORDS:** Redundant articulated robot (RAR); Nanocomposites; MWCNT; Dynamic performance; SolidWorks; SimMechanics; Mechanics explorer

## 1. Introduction

In robot design, material plays a vital role in enhancing its overall properties such as strength, stiffness, damping coefficient, corrosion resistance, wear resistance and low manufacturing cost. The materials such as aluminium alloy, magnesium alloy, titanium alloy, polymer matrix and metal matrix composites were used in robotics during the past few decades. Apart from other alloys, aluminium alloys were used by robot manufacturing industries due to its less weight, strength to weight ratio with low cost and high durability. The compact joints of the humanoid robots are made of titanium and 7075 aluminium alloys. The fatigue test was conducted by engaging polyether ether ketone (PEEK) with titanium alloy and then with 7075 aluminium alloy crank shafts of the robot joints.<sup>1</sup> The moving parts of articulated robot were made out of aluminium alloy 6061-T6 material by a researcher earlier due to low cost, good resistance to corrosion and workability.<sup>2</sup>

The composite structures are innovatively applied to components of robots considering the issues in the stiffness of composites.<sup>3</sup> The fast manoeuvrability and accuracy in positioning can be achieved by using robot material having high density and specific stiffness. The robot structural vibration can be dissipated if material damping is high. It cannot be attained using materials such as steel and aluminium. These materials have more or less similar specific stiffness and low damping property which are not adequate for robot structure. But composites have high specific stiffness, specific modulus and material damping.<sup>4</sup>

\* Corresponding author. E-mail: [saravana.moha@gmail.com](mailto:saravana.moha@gmail.com)

To improve further in terms of strength to weight ratio and its properties, reinforcement materials are selected in the nano-size level. The nano-size material will not influence much in terms of weight, rather it improves the properties of the material with respect to the manufacturing method selected to fabricate the nanocomposites. In recent decades, carbon-based reinforcement materials are widely developed, and carbon nanotubes (CNT) have very high aspect ratio and good mechanical stiffness due to their graphite structure.<sup>5-7</sup> CNT are classified into different types. Compared to other types, multiwalled carbon nanotubes (MWCNT) are widely used in industrial applications. MWCNT have high tensile strength and young's modulus properties, which influenced and made a revolution in the field of polymer matrix composites.<sup>8</sup>

The use of aluminium alloy 5083 (AA5083) in aerospace, missile, LNG tanks, offshore structure and marine applications was due to its corrosion resistance and strength to weight ratio. Many researchers fabricated CNT-based aluminium alloy (pure aluminium, AA2024, AA7075, A356, AA5083, AA6061) composites using rheological and squeeze casting, ball milling, sintering, hot isostatic pressing and spark plasma sintering for homogenous dispersion of CNT into the aluminium alloy.<sup>9-15</sup> The previous researchers' work shows that the addition of CNT into aluminium alloys increases tensile strength, young's modulus, hardness, wear resistance and impact strength based on CNT weight (or) volume fraction. This has led to add MWCNT as reinforcement into aluminium metal matrix composites (AMMCs) and implement in redundant articulated robot (RAR) components. The articulated robot is generally called as industrial robot with revolute revolute revolute (RRR) configuration with a limited working envelope,<sup>16</sup> in which the steel is used for the non-movable and aluminium for movable parts.

The redundant manipulators are dexterous and capable of doing versatile tasks than non-redundant manipulators. It is applicable for heavy duty purposes such as arc welding, spot welding, materials handling, machine tending, painting, picking, packing and palletizing, assembly, mechanical cutting, grinding, deburring and polishing, gluing, adhesive sealing and spraying materials inspection, waterjet cutting and soldering.<sup>17</sup>

In this work, RAR is proposed to test the effect of composite material characteristics. Earlier various research works were conducted to quantify the dexterity of robotic manipulators using simulation techniques and pave the way for its development.<sup>18-25</sup> The extensive literature survey reveals that the modelling and simulation is an advanced mechatronics method of analysing different mechanical and electromechanical system movements. The modelling and predominant simulation techniques pave the way for developing sophisticated electromechanical systems like the robots to meet the present day demand.

The need of modelling and advanced simulation techniques is indispensable to build a robot systems in a short time rapidly with less cost.<sup>26-28</sup> Prior to making a robot, it is much needed to design, test and predict its characteristics to solve many problems.<sup>29</sup> The mathematical simulation was used to measure the performance of hybrid articulated robot with two flexible links and six joints which was controlled by feed forward controller and a linear proportional derivative (PD) joint controller.<sup>30</sup> The physical reliable parameter configurations of each pose of the 6-axis articulated robot were identified using independent simulation models.<sup>31</sup>

The MATLAB and Robot Studio are used to simulate the model derived for ABB IRB 140 industrial manipulator by the investigators to achieve the solution.<sup>32</sup> The mathematical and software advancements are desirable for competent simulation of mechanical systems in the MATLAB/Simulink simulation environment.<sup>33</sup> The MATLAB SimMechanics is a prominent simulation tool in the development of robots. The modelling and simulation of mechanical and electromechanical systems were done using SimMechanics, and performance was analysed by eminent authors.<sup>34-40</sup>

The synergic combination SolidWorks and MATLAB Simulink/SimMechanics was utilised for modelling and simulation of lower extremity exoskeleton for rehabilitation. The dynamic and kinematic parameters are identified and also the stability analysis enables the robots structural modification with great ease.<sup>41</sup> The motion trajectory and the dynamic performance and the motion of 6 DOF spatial parallel robots, 3-RPS (Revolute Prismatic Spherical) parallel robot, two-link planar robot arm, 3-RRRT (Revolute Revolute Revolute Twist) parallel manipulator, SCARA robot, 3-RRR parallel robot were analysed using SimMechanics.<sup>42-46</sup>

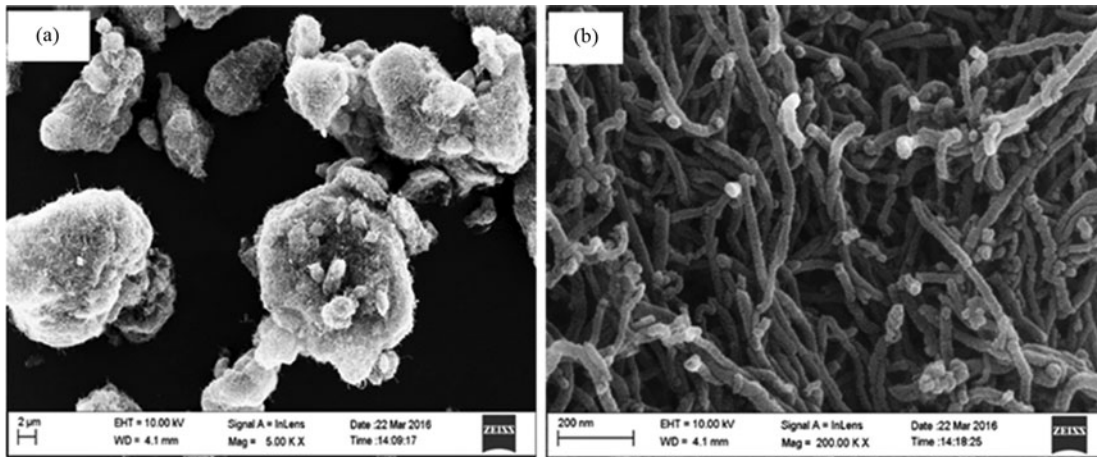


Fig. 1. (a) Field-emission scanning electron microscope (FE-SEM) image of multiwalled carbon nanotube (MWCNT) CVD processed (Mag = 5.00 KX); (b) multiwalled carbon nanotube (MWCNT) CVD processed (Mag = 200.00 KX).

A prototypical industrial spot welding robot was developed using SimMechanics, and the simulation was performed by the researchers.<sup>47</sup> The simulation accurately predicted the motion parameters and path of the robot. The 3D CAD model of KUKA KR5 robot for peg-in-hole insertion was developed using Autodesk Inventor and simulation using MATLAB/SimMechanics. This methodology was used to verify the inverse dynamics of the robot.<sup>48</sup> To improve the inspection speeds of KUKA KR16 L6-2 robot for non-destructive testing (NDT) in aerospace parts, MATLAB toolbox ROBONDT was developed for NDT which was capable of simulating the complex path planning, obstacle avoidance and external synchronisation.<sup>49</sup> The EON studio and MATLAB modelling and simulation technique were used to analyse and identify the control functions of 6R robot.<sup>50</sup>

The SolidWorks modelling software is very efficient tool in mechanical systems product development. Utilizing its compatibility with other prominent simulation software like MATLAB paves the way for developing complicated electromechanical systems like robots. The 4 DOF of robotic arm for roselle tea process plant was modelled and simulated using the SolidWorks and MATLAB/Simulink to analyse its dynamic and static performance.<sup>51</sup> Four-axis industrial robot with its parts assigned with additive manufacturing technology powder material applicable for palletising was earlier simulated and analysed using solid works and MATLAB/SimMechanics.<sup>52</sup>

In this work, the influence of MWCNT-reinforced alloy AA5083 in RAR design has been studied in five stages. First, multiwalled-carbon nanotube is reinforced with the aluminium alloy 5083 (AA5083) using semi-solid state stir casting process developed nanocomposites for four varying compositions. Second, the mechanical and damping properties of the nanocomposite developed materials were experimentally tested and observed. Third, the corresponding material property values are assigned to the 3D CAD model of the RAR arms with the aid of modelling software SolidWorks. In the fourth stage, the multi body system block diagram of the robot was developed by exporting the CAD model to SimMechanics environment, and simulation was conducted to observe the torque in the manipulator joints.

## 2. Material Design

The MWCNT particles mixed with AA5083 matrix material by varying compositions like 0 and 1.75 by the weight fraction using stir casting method. The matrix material was added as billets into the graphite crucible and melted at 560°C to 590°C for 210 min into semi-solid state (compo-casting). The preheated MWCNT was mixed along with the matrix material in a semi-solid state phase and stirred at 260 rpm for 2.5 min to obtain a uniform dispersion of MWCNT into the AA5083 material. The mixed AA5083-MWCNT material was poured into a split die to obtain a nanocomposite material. Similar routes are followed for other compositions and developed the MWCNT-reinforced aluminium matrix nanocomposites.

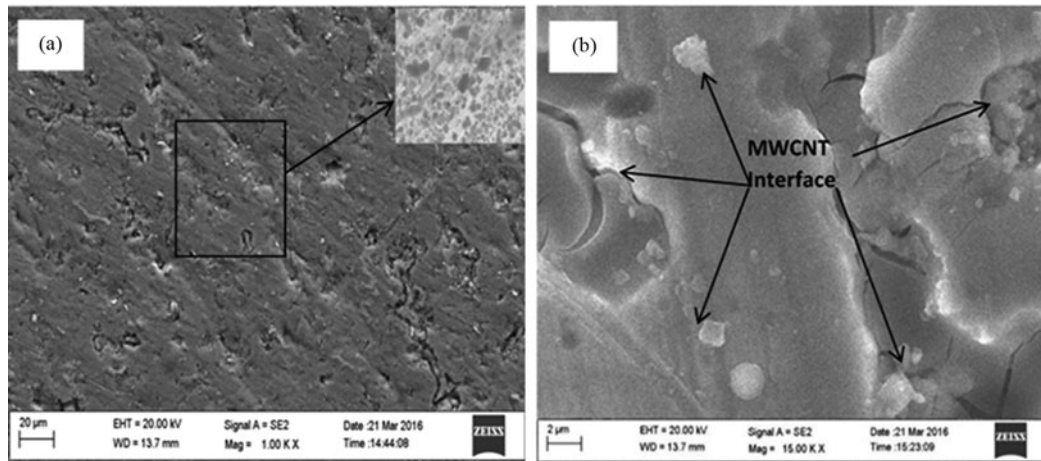


Fig. 2. (a) Field-emission scanning electron microscope (FE-SEM) image of AA5083 material; (b) AA5083 – 1.75 wt% of MWCNT.

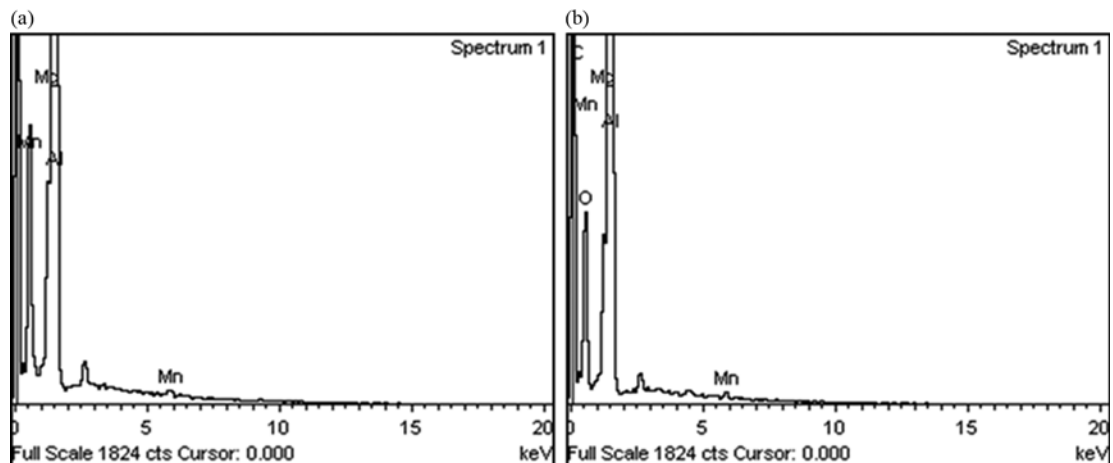


Fig. 3. (a) EDX image of AA5083 alloy; (b) AA5083 – 1.75 wt% of MWCNT.

Field emission scanning electron microscope (FE-SEM) examined images of MWCNT – CVD processed with lower magnification (Mag = 5.00KX) is shown in Fig. 1a and with higher magnification (Mag = 200.00KX) in Fig. 1b.

FE-SEM secondary electron (SE) image of developed AA5083 is shown in Figure 2(a), and nanocomposite with varying weight fraction of MWCNT is shown in Figure 2(b). In the case of 1.75 weight fraction, MWCNT dispersion is uniform into the matrix material, as same as the examined images of MWCNT shown in Figure 2a. A minimum level of cluster formation of MWCNT was observed in 1.75 weight fraction, as shown in Figure 2b.

The EDX images of AA5083 and AA5083/MWCNT nanocomposites were shown in Figure 3(a,b). Figure 3(a) shows the peak that lies between the range of 1–3, which shows the presence of base elements such as Al, Mg and Mn in the matrix material. Figure 3(b) indicates excess elements such as C and O in the matrix material at the range of 0–1. The peak value of elements C and O indicates the presence of CNT in the matrix material without any excess metal particles.

### 3. Mechanical and Dynamic Property Test

As per ASTM A370, tensile specimens with a gauge length of 32 mm, height of 10 mm and thickness of 5 mm were used. The specimens were machined using a Wire EDM machine. The tensile tests were carried out in TUV Rheinland (India) Pvt. Ltd., Coimbatore. Based on ASTM B311-08, density was measured using a water displacement approach (Archimedean density), and Brinell hardness test was carried out based on ASTM E10.<sup>39</sup> The ultimate tensile strength of 0, 0.5, 1, 1.5 weight fraction

Table I. Mechanical properties of AA5083 and MWCNT-reinforced composites.

Material used in weight %	Density (g/cm <sup>3</sup> )	Percentage increase (%)	Tensile strength (MPa)	Percentage increase (%)	Hardness (BHN)	Percentage increase (%)
AA5083	2.693	–	168.23	–	74	–
AA5083 – 1.75% MWCNT	2.736	1.59	234.00	39.09	84	13.51

Table II. Modified material versus dynamic parameter.

Link dimensions	$l_1 = 250\text{mm}, l_2 = 250\text{mm}, l_3 = 350\text{mm},$ $l_4 = 250\text{mm}, l_5 = 100\text{mm}, l_6 = 100\text{mm}$			
	Materials used	AA5083	AA5083 – 1.75% MWCNT	Percentage variation in joint torque (%)
		Joint torque (Nm)		
Joint 1		683	693.9	1.59
Joint 2		4885	4961	1.55
Joint 3		2200	2234	1.54
Joint 4		1423	1445	1.26
Joint 5		142.8	144.9	1.47
Joint 6		64.35	65.29	1.46
Joint 7		1.213	1.214	0.08

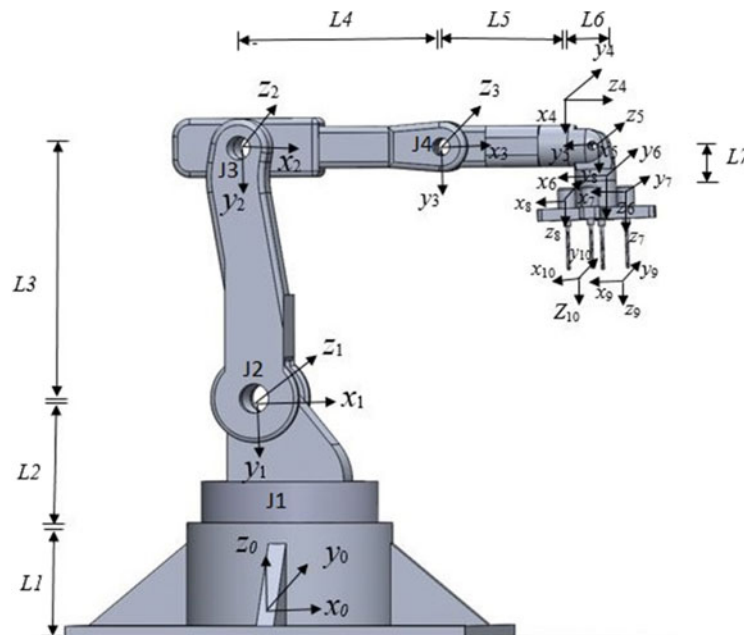


Fig. 4. SolidWorks model of RAR with axis convention.

of MWCNT reinforced with pure aluminium/AA5083 developed using the ball milling method<sup>9,14</sup> was observed in earlier research works. In this present work, 1.75 wt% MWCNT is experimented using compo-casting method and observed the increase in ultimate tensile strength. Table I shows the ultimate tensile strength (UTS), density and hardness value of AA5083 and AA5083/MWCNT composites.



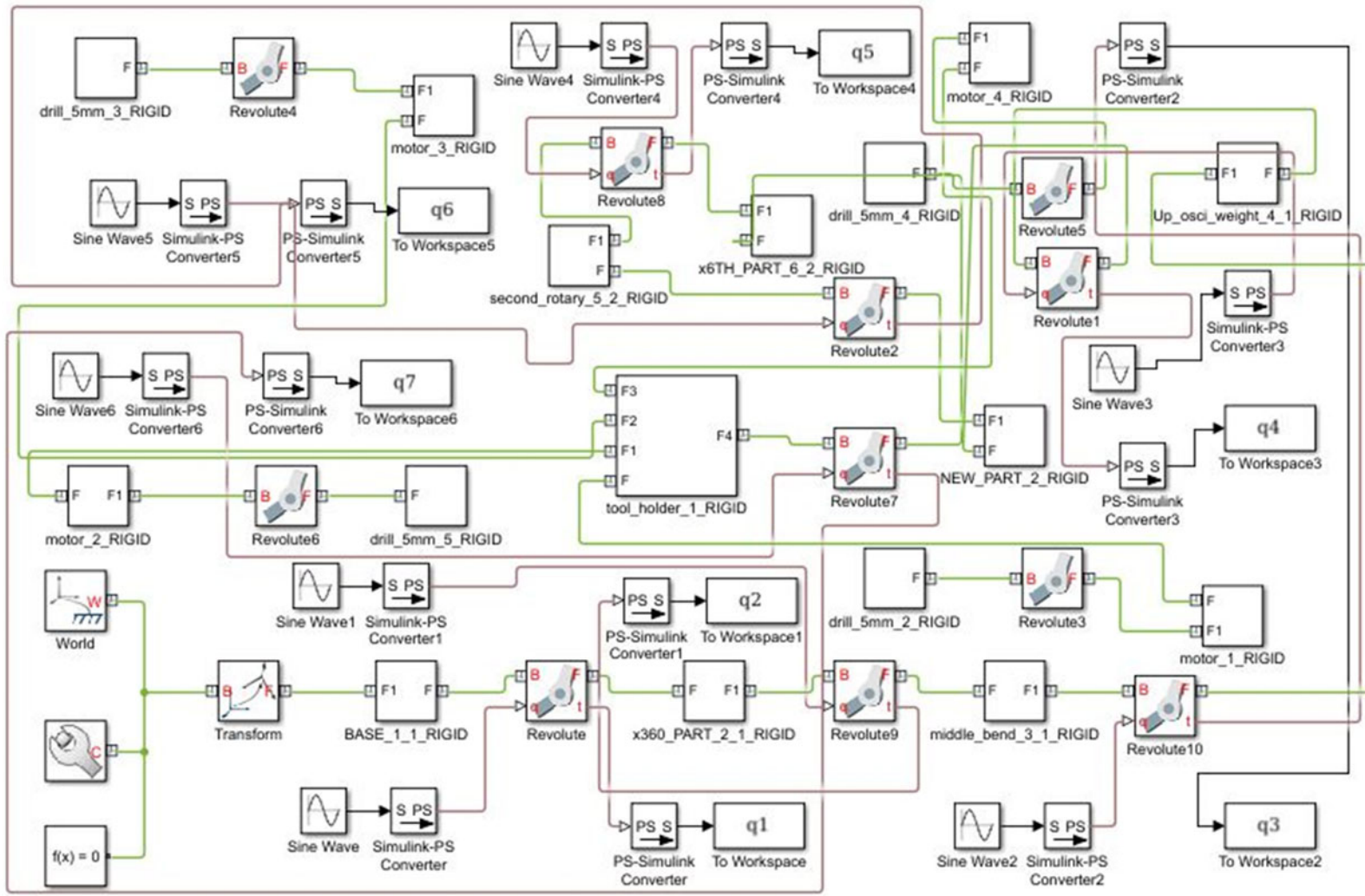


Fig. 5. SimMechanics block diagram to find the torque at revolute joints.

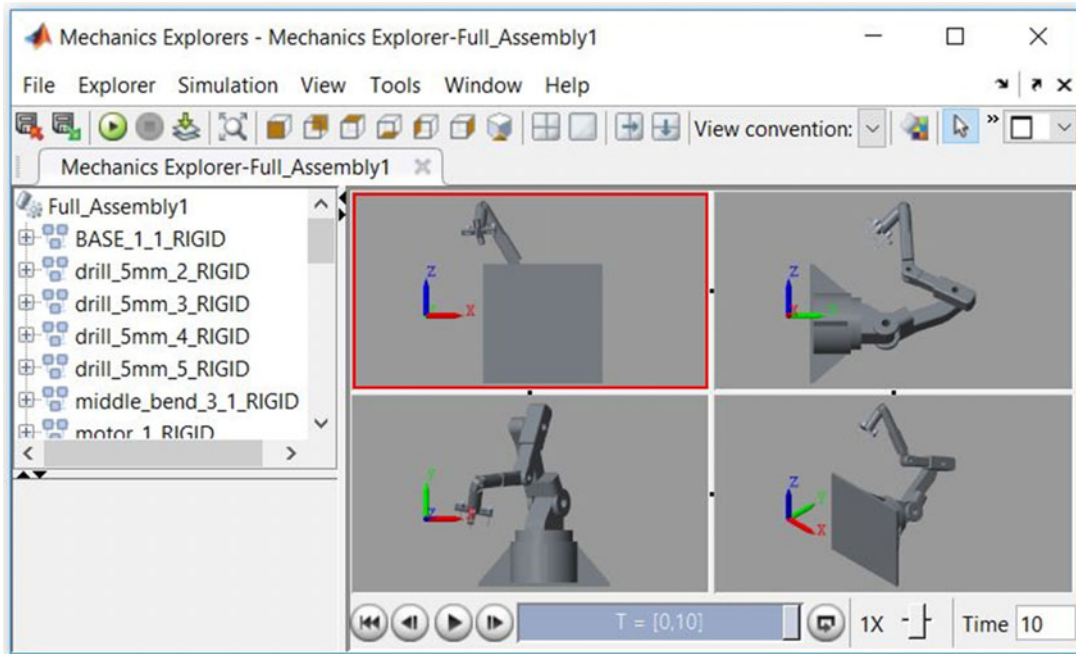


Fig. 6. SimMechanics explorer view of the RAR simulation.

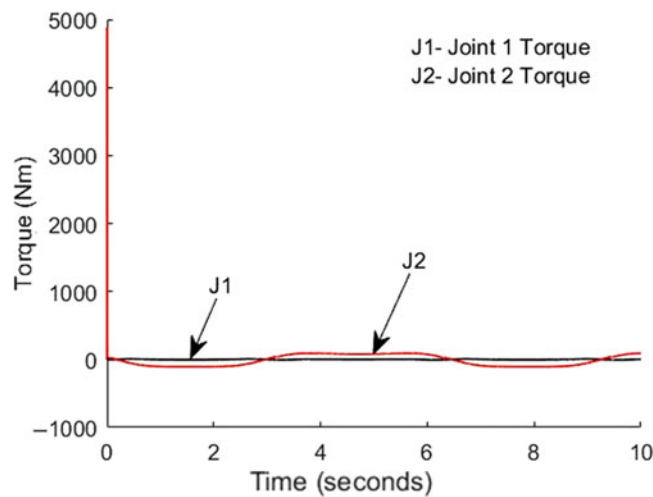


Fig. 7. Torque of revolute joint 1 and joint 2 if material is AA5083 – 0% MWCNT.

**4. Modelling by SolidWorks**

SolidWorks is a solid modelling software which is used to produce parts and assembly drawings by utilising parametric features. Here parameters are referred to constraints. Its values determine the shape or geometry of the model. Using this CAD modelling software, the newly proposed RAR of its kind with MTEE is modelled. This RAR model comprises of revolute joints. The tool head is attached to the prismatic arm in its bottom that is capable of holding four drilling tools placed mutually perpendicular as shown in Figure 4. The material assigned to the parts and the required design parameters of RAR are mentioned in Table II.

**5. SimMechanics Simulation**

SimMechanics is a virtual reality with multibody system environment for three-dimensional machine-driven and electromechanical systems. The CAD model is used by the SimMechanics to generate and solve the motion equation of the multibody system. It is modelled in the form of sequence of blocks symbolising bodies, constraints, joints and force elements as shown in Figure 5.

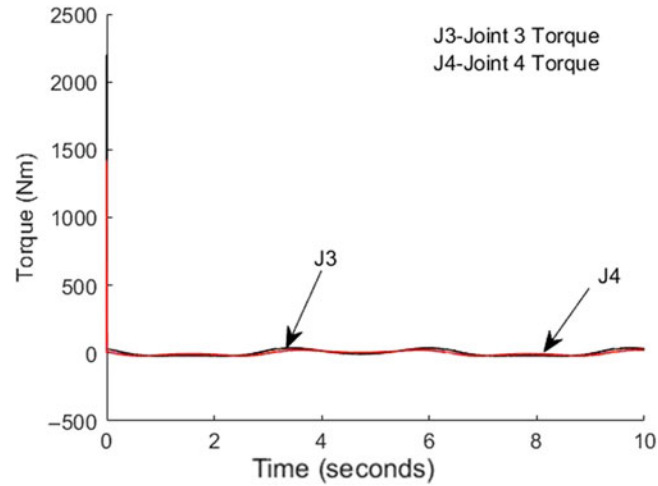


Fig. 8. Torque of revolute joint 3 and joint 4 if material is AA5083 – 0% MWCNT.

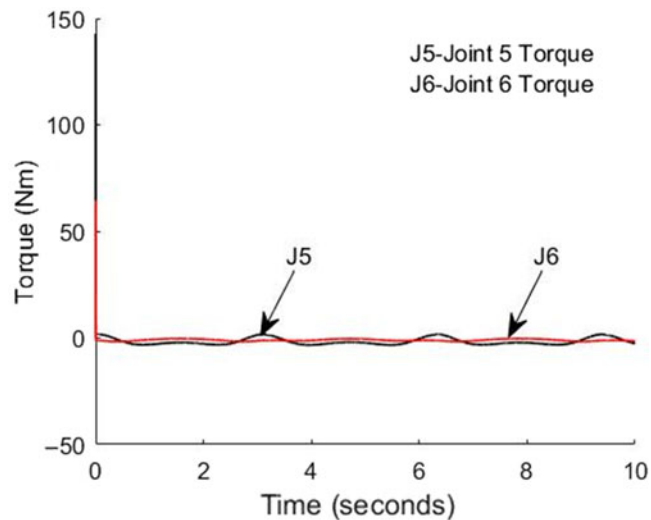


Fig. 9. Torque of revolute joint 5 and joint 6 if material is AA5083 – 0% MWCNT.

SimMechanics has the capability to vary the structure with optimised system constraints and also the simulation results can be analysed in much lesser time.

In this work, the 3D CAD model of the proposed redundant robot was exported to MATLAB/SimMechanics through SimMechanics made available in the SolidWorks modelling platform. The XML file obtained by the export operation is executed in the SimMechanics second-generation environment. This process obtains the multibody system block diagram with interlinked blocks signifying the rigid body links and joints. The required joint primitives are assigned to the joint blocks to get the actuator performance output. The 3D animation in the MATLAB/SimMechanics Explorer window exposed the robotic system dynamics as shown in Figure 6. In this section, the dynamic parameter torque in the robotic manipulator joints is observed by applying SimMechanics second-generation simulation technique.

## 6. SimMechanics Simulation Results

The MWCNT-reinforced material 0% MWCNT and 1.75% MWCNT assigned as a custom material to the links of the RAR CAD model, and simulation was carried out on SimMechanics platform through which the dynamic parameter torque was observed. The dynamic parameter, torque with respect to the material assigned to the manipulator links, is listed in Table II.



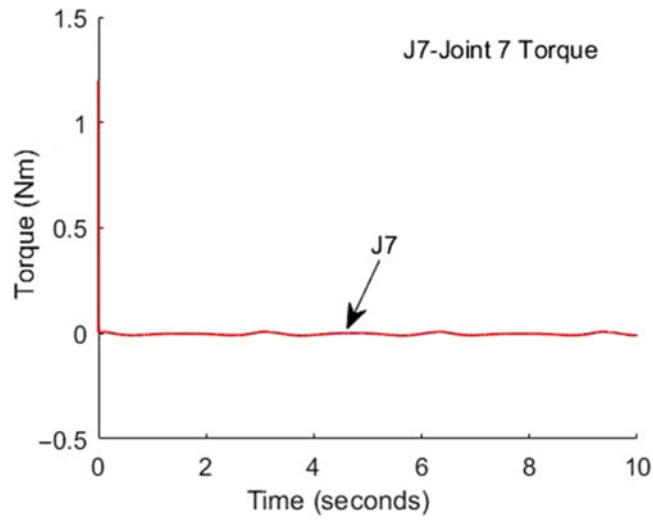


Fig. 10. Torque of revolute joint 7, if material is AA5083 – 0% MWCNT.

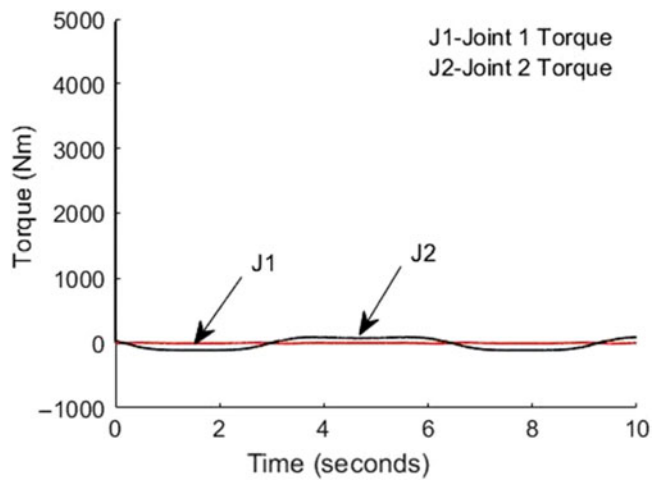


Fig. 11. Torque of revolute joint 1 and joint 2, if material is AA5083 – 1.75% MWCNT.

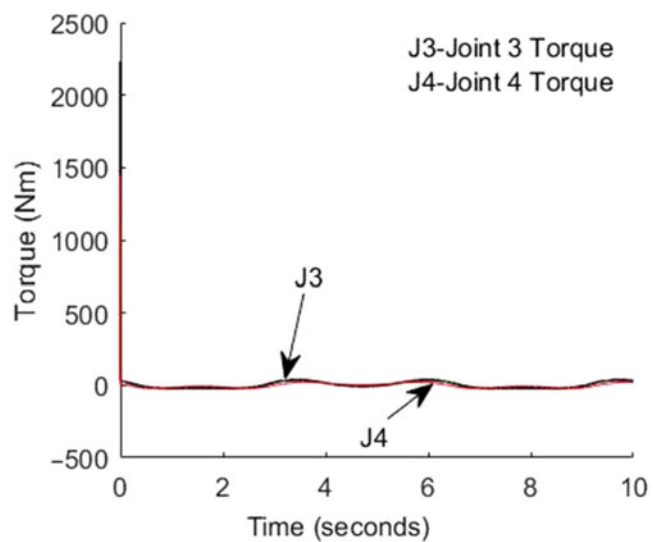


Fig. 12. Torque of revolute joint 3 and joint 4, if material is AA5083 – 1.75% MWCNT.

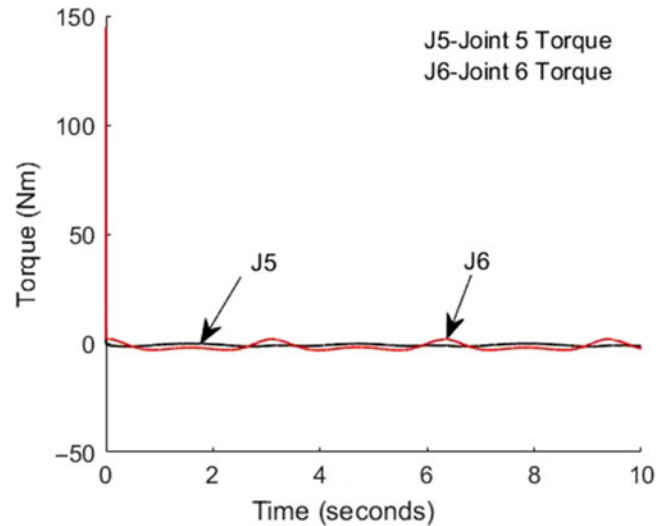


Fig. 13. Torque of revolute joint 5 and joint 6, if material is AA5083 – 1.75% MWCNT.

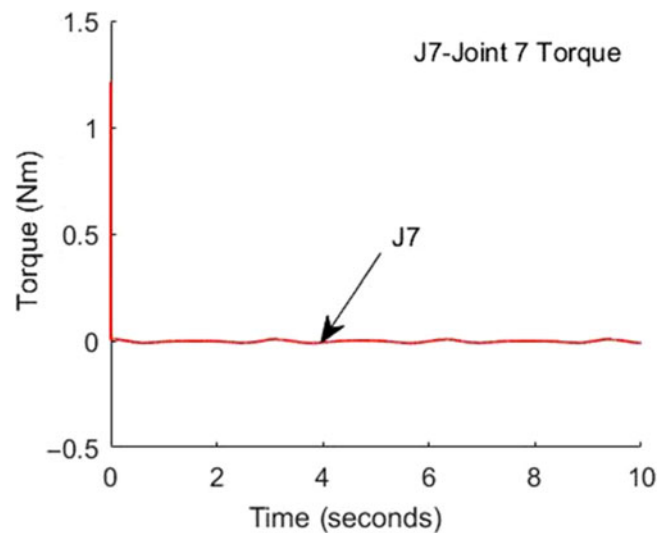


Fig. 14. Torque of revolute joint 7, if material is AA5083 – 1.75% MWCNT.

To obtain filtered torque output, it is required to add the appropriate Simulink – PS convertor and sine wave blocks as the input to the actuator and PS-Simulink convertor along with the workspace with the output port in the SimMechanics block diagram. The joint torque sensing primitives are then enabled to get the filtered torque output in the form of the graph shown in Figures 6–13 through the workspace for time instant  $t = 10$  s. The MATLAB Explorer window shows the simulated path of the robotic manipulator, as shown in Fig. 6.

Figs. 7 and 8 illustrate the torque at joint 1, joint 2, joint 3 and joint 4, if AA5083 – 0% CNT is assigned to the robot links. The torque values observed are 683, 4885, 2200 and 1423 Nm.

Figs. 9 and 10 indicate the joint 5, joint 6 and joint 7 torque values as 142.8, 64.35 and 1.21 Nm, if AA5083 – 0% CNT is assigned to the robotic manipulator links.

The torque at joint 1, joint 2, joint 3 and joint 4 is 693.9, 4961, 2234 and 1445 Nm is shown in Figs. 11 and 12, if the material used is AA5083 – 1.75% MWCNT in the robot links.

If the material assigned to the manipulator link is AA5083 – 1.75% MWCNT, the torque in the joint 5, joint 6, and joint 7 is observed as 144.9, 65.29 and 1.214, as shown in Figs. 13 and 14.

The torque observed in the revolute joints of redundant robotic manipulator for modified CNT-reinforced material 0% MWCNT and 1.75% MWCNT are listed in Table II. The addition of 1.75% MWCNT in AA5083 shows less than 5% increase in the joint torque values.

## 7. Conclusions

In this paper, the influence of CNT-based nanocomposite properties on dynamic performance of RAR is studied by applying Solidworks CAD modelling and MATLAB/SimMechanics simulation technique. The CAD model of the proposed RAR was imported into the MATLAB – II gen. environment, and simulation was performed to observe the joint torque dynamic parameter of the RAR manipulator. The simulation results of robotic manipulator design provide varying torque values for the modified aluminium nanocomposite material. The 1.75 weight fraction MWCNT of aluminium nanocomposite shows better mechanical property than the AA5083 material. It is observed that the dynamic performance of RAR vary with modified design material. The difference in the torque values is minimal and it is considered to be in acceptable limit. It is appropriate to apply AA5083 – 1.75 weight fraction MWCNT as the material for fabricating the links of the RAR manipulator.

## References

1. I. Kiyoto, K. Hitonobu, K. Katsuyuki, K. Kenji, "Observation of wear surface between pure PEEK and counterpart materials; titanium and 7075 aluminum alloy, in robot joint," *App. Mech. Mater.* **307**, 347–351 (2013).
2. D. R. Dentler II, Design, Control, and Implementation of a Three Link Articulated Robot Arm. *Master's Thesis* (Dept. Mechanical. Eng. Akron (OH): The University of Akron, 2008).
3. G. L. Dai, S. L. Chang, G. L. Hak, Y. H. Hui and W. K. Jong, "Novel applications of composite structures to robots, machine tools and automobiles," *Comp. Struc.* **66**(1–4), 17–39 (2004).
4. G. L. Dai, S. J. Kwang, S.K. Ki and K. K. Yoon, "Development of the anthropomorphic robot with carbon fiber epoxy composite materials," *Comp. Struc.* **25**(1–4), 313–324 (1993).
5. Q. Li and A. Christian, "CNT reinforced light metal composites produced by melt stirring and by high pressure die casting," *Comp. Sci. Tech.* **70**(16), 2242–2247 (2010).
6. E. T. Thostenson, C. Li and T. W. Chou, "Nanocomposites in context," *Comp. Sci. Tech.* **65**(3–4), 491–516 (2005).
7. C. Li and T. W. Chou, "Elastic moduli of multi-walled carbon nanotubes and the effect of van der Waals forces," *Comp. Sci. Tech.* **63**(11), 1517–1524 (2003).
8. K. T. Kashyap and R. G. Patil, "On Young's modulus of multi-walled carbon nanotubes," *Bull. Mater. Sci.* **31**, 185–187 (2008).
9. A. Esawi, K. Morsi and A. Sayed, "Effect of carbon nanotube (CNT) content on the mechanical properties of CNT-reinforced aluminium composites," *Comp. Sci. Tech.* **70**(16), 2237–2241 (2010)
10. Z. Y. Liu, S. J. Xu and B. L. Xiao, "Effect of ball-milling time on mechanical properties of carbon nanotubes reinforced aluminium matrix composites," *Comp. Part A* **43**(12), 2161–2168 (2012).
11. J. Liao and M. J. Tan, "A simple approach to prepare Al/CNT composite: spread–dispersion (SD) method," *Mater. Lett.* **65**(17–18), 2742–2744 (2011).
12. H. J. Choi, J. H. Shin and D. H. Bae, "The effect of milling conditions on microstructures and mechanical properties of Al/MWCNT composites," *Comp. Part A* **43**(7), 1061–1072, (2012).
13. S. E. Shin and D. H. Bae, "Strengthening behavior of chopped multi-walled carbon nanotube reinforced aluminum matrix composites," *Mater. Charac.* **83**, 170–177 (2013).
14. P. S. Samuel Ratna Kumar, D.S. Robinson Smart and S. John Alexis, "Corrosion behaviour of aluminium metal matrix reinforced with multi-wall carbon nanotube," *J. Asian Ceram. Soc.* **5**(1), 71–75, (2017).
15. B. Chen and J. Shen, "Solid-state interfacial reaction and load transfer efficiency in carbon nanotubes (CNTs)-reinforced aluminum matrix composites," *Carbon.* **114**, 198–208 (2017).
16. B. Siciliano and O. Khatib, *Handbook of Robotics* (Springer, Berlin, Heidelberg, 2008).
17. R. Patel and F. Shadpey, *Control of Redundant Robot Manipulators* (Springer Verlag, Berlin, Heidelberg, 2005).
18. A. Maciejewski and C. A. Klein, "Obstacle avoidance for kinematically redundant manipulators in dynamically varying environments," *Int. J. Robot. Res.* **4**(3), 109–119 (1985)
19. Y. Nakamura, H. Hanafusa and T. Yoshikawa, "Task-priority based redundancy control of robot manipulators," *Int. J. Robot. Res.* **6**(2), 3–15 (1987).
20. C. A. Klein and B. E. Blaho, "Dexterity measures for the design and control of kinematically redundant manipulators," *Int. J. Robot. Res.* **6**(2), 72–84 (1987).
21. H. Seraji, "Improved configuration control for redundant robots," *J. Robot. Syst.* **7**(6), 897–928 (1990).
22. A. Maciejewski, "Kinetic limitations on the use of redundancy in robotic manipulators," *IEEE Trans. Robot. Autom.* **7**(2), 205–211 (1991).
23. V. Potkonjak, "New approach to the application of redundant robots," *Robot. Comput. Integ. Manuf.* **8**(3), 181–185 (1991).
24. C. L. Chen and C. J. Lin, "Motion planning of redundant robots," *J. Robot. Syst.* **14**(12), 839–850 (1997).
25. G. C. Vosniakos and Z. Kannas, "Motion coordination for industrial robotic systems with redundant degrees of freedom," *Robot. Comput. Integ. Manuf.* **25**(2), 417–431 (2009).
26. O. Michel, "Cyberbotics Ltd – WebotsTM: Professional mobile robot simulation," *Int. J. Adv. Robot. Syst.* **1**(1), 39–42 (2004).

27. L. Zlajpah, "Simulation in robotics," *Math. Comput. Simulat.* **79**(4), 879–897 (2008).
28. Z. Sika, M. Valasek, V. Bauma and T. V. Ampola, "Design of redundant parallel robots by multidisciplinary virtual modeling," In: *Virtual Nonlinear Multibody Systems* (W. Schiehlen and M. Valasek, eds.) (Kluwer Academic Publishers, Dordrecht, 2003) pp. 233–241.
29. F. Ionescu, "Modelling and simulation in mechatronics," *IFAC Proc.* **40**(18), 301–312 (2007).
30. W. Hobarth, H. Gattringer and H. Bremer, "A dynamic model for a hybrid articulated robot," *Proc. Appl. Math. Mech.* **8**(1) 10123–10124 (2008).
31. J. Fleischera and M. Kraußeb, "Physically consistent parameter optimization for the generation of pose independent simulation models using the example of a 6-axis articulated robot," *Procedia CIRP* **12**, 217–221 (2013).
32. M. Almagad, "Forward and inverse kinematic analysis and validation of the ABB IRB 140 industrial robot," *Int. J. Electron. Mech. Mechatron. Eng.* **7**(2), 1383–1401 (2017).
33. G. D. Wood and D. C. Kennedy, *Simulating Mechanical Systems in Simulink with SimMechanics* (The MathWorks, Natick 2003). Available from: Math works [06 January 2016].
34. Y. Shaoqiang, L. Zhong and L. Xingshan, "Modeling and Simulation of Robot Based on Matlab/SimMechanics." *Proceedings of the 27th Chinese Control Conference, Yunnan, China*, (2008) pp. 161–165.
35. L. Z. Wen, Z. G. Liang, Z. W. Ping and J. Bin, "A simulation platform design of humanoid robot based on SimMechanics and VRML," *Procedia Eng.* **15**, 215–219 (2011).
36. M. Fajar, S. S. Douglas and J. B. Gomm, "Modelling and simulation of spherical inverted pendulum based on LQR control with SimMechanics," *Appl. Mech. Mater.* **391**, 163–167 (2013).
37. M. E. Kutuk, R. Halicioglu and L. C. Dulger, "Kinematics and simulation of a hybrid mechanism: MATLAB/SimMechanics," *J. Phys. Conf. Ser.* **574**, 451–458 (2015).
38. B. Zi, J. Cao and Z. Zhu, "Dynamic simulation of hybrid-driven planar five bar parallel mechanism based on SimMechanics and tracking control," *Int. J. Adv. Robot. Syst.* **8**(4), 28–33 (2011).
39. J. Liu, Y. Gong, G. Chen and H. Chen, "Modeling and Simulation of Loader Working Device Based on SimMechanics," *International Conference on Transportation, Mechanical, and Electrical Engineering (TMEE), Changchun, China* (2011) pp. 2054–2059.
40. L. Yu, L. Zhang, N. Zhang and S. Yang, "Kinematics, simulation and analysis of 3-RPS parallel robot on SimMechanics," *Proc. IEEE Int. Conf. Inf. Autom.* (2010) pp. 2363–2367.
41. Y. Li, X. Wang, P. Xu, D. Zheng, W. Liu, Y. Wang and H. Qiao, "SolidWorks/SimMechanics Based Lower Extremity Exoskeleton Modeling Procedure for Rehabilitation," *World Congress on Medical Physics and Biomedical Engineering, IFMBE Proceedings* (2013) pp. 2058–2061.
42. C. Yang, J. He, J. Han and X. Liu, "Real-time state estimation for spatial six-degree-of-freedom linearly actuated parallel robots," *Mechatronics* **19**(6), 1026–1033 (2009).
43. L. Hanchen, Z. Xinhua and X. Haoliang, "Modelling and simulation of 3RRRT parallel manipulator based on MALTAB with SimMechanics," *Proc. Int. Forum Inf. Technol. App.* (2009) pp. 290–293.
44. M. Gouasmi, M. Ouali, B. Fernini and M. Meghatria, "Kinematic modelling and simulation of a 2-R robot using SolidWorks and verification by MATLAB/Simulink," *Int. J. Adv. Robot. Syst.* **9**(6), 245 (2012).
45. M. Saravanamohan and V. Anbumalar, "Modelling and simulation of multi spindle drilling redundant SCARA robot using SolidWorks and MATLAB/SimMechanics," *RevistaFacultad de Ingeniería*, **8**(1), 63–72 (2016).
46. J. Gao, Y. Wang and Z. Chen, "Modelling and simulation of inverse kinematics for planar 3-RRR parallel robot based on SimMechanics," *Adv. Mat. Res.* **898**, 510–513 (2014).
47. L. S. Gang, D. H. Wang, W. S. Cheng and Z. Y. Nan, "Path planning and system simulation for an industrial spot welding robot based on SimMechanics," *Key Eng. Mat.* **419-420**, 665–668 (2010).
48. A. D. Udai, C. G. Rajeevlochana and S.K. Saha, "Dynamic Simulation of a KUKA KR5 Industrial Robot Using MATLAB SimMechanics," *15th National Conference on Machines and Mechanisms (NaCoMM) 2011, Chennai, India* (2011) pp. 1–8.
49. C. Mineo, S. G. Pierce, P. I. Nicholson and I. Cooper, "Robotic path planning for non-destructive testing – a custom MATLAB toolbox approach," *Robot. Comput. Integr. Manuf.* **37**, 1–12 (2016)
50. W. Juan, S. Z. He, Z. Z. Xiang and M. E. Rong, "Analysis and simulation of 6R robot in virtual reality," *IFAC Papers OnLine* **49**(16), 426–430 (2016).
51. M. K. Adeyeri, S. P. Ayodeji and O. Olasanoye, "Modelling and simulation of 4 DOF robotic arm for an automated Roselle tea processing plant using Solidwoks and Matlab Simulik," *IFAC PapersOnLine*, **50**(2), 249–250 (2017).
52. M. Aburaia, E. Markl and K. Stuja, "New concept for design and control of 4 axis robot using the additive manufacturing technology," *Procedia Eng.* **100**, 1364–1369 (2015).